Published in final edited form as:
Hear Res. 2013 December ; 306: 93–103. doi:10.1016/j.heares.2013.09.014.

ECAP Spread of Excitation with Virtual Channels and Physical Electrodes

Michelle L. Hughes, **Lisa J. Stille**, **Jacquelyn L. Baudhuin**, and **Jenny L. Goehring**
Boys Town National Research Hospital Lied Learning and Technology Center 425 North 30th Street Omaha, Nebraska 68131

Abstract

The primary goal of this study was to evaluate physiological spatial excitation patterns for stimulation of adjacent physical electrodes and intermediate virtual channels. Two experiments were conducted that utilized electrically evoked compound action potential (ECAP) spread-of-excitation (SOE) functions obtained with the traditional forward-masking subtraction method. These two experiments examined spatial excitation patterns for virtual-channel maskers and probes, respectively. In Experiment 1, ECAP SOE patterns were obtained for maskers applied to physical electrodes and virtual channels to determine whether virtual-channel maskers yield SOE patterns similar to those predicted from physical electrodes. In Experiment 2, spatial separation of SOE functions was compared for two adjacent physical probe electrodes and the intermediate virtual channel to determine the extent to which ECAP SOE patterns for virtual-channel probes are spatially separate from those obtained with physical electrodes. Data were obtained for three electrode regions (basal, middle, apical) for 35 ears implanted with Cochlear (N = 16) or Advanced Bionics (N = 19) devices. Results from Experiment 1 showed no significant difference between predicted and measured ECAP amplitudes for Advanced Bionics subjects. Measured ECAP amplitudes for virtual-channel maskers were significantly larger than the predicted amplitudes for Cochlear subjects; however, the difference was <2 μV and thus is likely not clinically significant. Results from Experiment 2 showed that the probe set in the apical region demonstrated the least amount of spatial separation amongst SOE functions, which may be attributed to more uniform nerve survival patterns, closer electrode spacing, and/or the tapered geometry of the cochlea. As expected, adjacent physical probes demonstrated greater spatial separation than for comparisons between each physical probe and the intermediate virtual channel. Finally, the virtual-channel SOE functions were generally weighted toward the basal electrode in the pair.

Keywords

cochlear implant; electrically evoked compound action potential; spread of excitation; virtual channels

Corresponding author: Michelle L. Hughes; 425 North 30th Street, Omaha, NE, 68131, USA; phone: 402-452-5038; fax: 402-452-5028; michelle.hughes@boystown.org.

1. Introduction

The restricted number of physical electrodes in a cochlear implant (CI) limits the amount of spectral information that can be represented by the device (e.g., Henry and Turner, 2003; Henry et al., 2005). Several methods to improve spectral representations have been investigated, including the use of "virtual channels" (e.g., Firszt et al., 2007; Kwon and van den Honert, 2006). Stimulation with virtual channels may recruit slightly different populations of neurons than those activated by individual physical electrode contacts. The theoretical advantage of creating additional regions of stimulation is improved spectral representation of the stimulus and potentially improved speech perception.

Virtual channels can be produced in several ways. Adjacent or closely-spaced electrodes that are sequentially stimulated within a very short time interval (<500 μsec) can produce pitch percepts that are different from those produced by each of the contributing electrodes in isolation (e.g., McDermott and McKay, 1994; McKay et al., 1996; Kwon and van den Honert, 2006). This method can be used with overlapping or bell-shaped filters, as utilized with Cochlear and MED-EL devices. Another technique, referred to as "dual electrode" stimulation (Busby and Plant, 2005; Busby et al., 2008), simultaneously stimulates two adjacent electrodes via electrical coupling. The result is a single "electrode" intended to recruit a slightly different population of neurons than when either physical electrode contact is stimulated exclusively. The newer-generation Cochlear devices, Nucleus 24RE "Freedom" (CI412, CI422) and CI512, have dual-electrode capabilities; however, this feature is currently not FDA approved for commercial use. Research has shown that distinguishable pitches can be perceived when using dual-electrode stimulation compared to when each of the contributing physical electrodes are stimulated alone (Busby and Plant, 2005; Busby et al., 2008). However, the precise location and shape of the electrical field cannot be controlled because only a single current source is used, and the resulting electrical field is dependent upon the relative impedance of the two contributing electrodes.

Finally, "current steering" uses separate current sources to stimulate two electrodes simultaneously, typically in phase (Firszt et al., 2007; Koch et al., 2007; Bonham and Litvak, 2008; Choi and Hsu, 2009; Frijns et al., 2009; Saoji et al., 2009). Pitch percepts can change as the ratio of total current is varied between the two physical electrodes because the shape of the summed electrical field changes, altering the resulting neural excitation patterns. Unlike Cochlear's dual-electrode mode, the use of individual current sources allows for greater control or "steering" of the location and shape of the electrical field. Advanced Bionics (AB) and MED-EL I^{100} devices both have independent current sources; however, AB is currently the only manufacturer that makes use of virtual channels in a clinical speech-processing strategy (Fidelity 120). AB devices that employ virtual-channel capabilities are the CII and 90K.

Neural spread-of-excitation (SOE) patterns measured with the electrically evoked compound action potential (ECAP) can be obtained with a forward-masking subtraction method in which the position of the probe and recording electrode are fixed and the masker electrode is varied across the array (e.g., Abbas et al., 1999, 2004; Busby et al., 2008; Hughes and Goulson, 2011). The resulting SOE function represents the neural excitation pattern elicited by the probe electrode. ECAP SOE functions for virtual-channel probe electrodes have been shown, on average, to be similar in width and shape to those obtained for the physical probe electrode contacts (Busby et al., 2008; Hughes and Goulson, 2011; Saoji et al., 2009). There is evidence, however, that ECAP amplitudes for virtual-channel stimulation are larger than for stimulation of the adjacent physical electrodes (Busby et al., 2008; Hughes and Goulson, 2011). Busby et al. (2008) showed that peak ECAP amplitudes for dual-electrode SOE functions were an average of 6% larger than for the flanking physical electrodes, and up to

10% larger for one of the basal pairs tested (the latter being statistically significant). It is therefore possible that amplitudes for virtual-channel *maskers* may be slightly larger than for physical electrodes, which could affect measures such as the width of the SOE pattern (e.g., Busby et al., 2008) or the spatial separation between SOE probe functions (as measured in Hughes, 2008). The effect of virtual-channel maskers for ECAP SOE patterns therefore requires further investigation.

It is also of interest to quantify the amount of spatial overlap of neural SOE patterns for physical versus virtual probe electrodes to examine the extent to which virtual-channel SOE patterns are spatially separate from physical-electrode SOE patterns (i.e. P10, P10+11, and P11, where "+" indicates the virtual channel). In a study by Hughes (2008), the spatial separation of SOE functions between pairs of physical probe electrodes (i.e. P9 and P11) was quantified as the cumulative difference in normalized ECAP amplitudes across all masker electrodes, termed the *ECAP separation index*[1]. Results indicated that the amount of spatial separation between the two physical electrodes correlated with the ability to perceptually distinguish between the electrodes on a pitch-ranking task. Specifically, greater accuracy in pitch ranking was strongly correlated with greater spatial separation of ECAP SOE functions. The present study extends the methodology used in the Hughes (2008) study to quantify the spatial separation of SOE patterns for virtual channels and adjacent physical electrode contacts for electrodes in the basal, middle, and apical regions. This study represents the first step in a series of experiments designed to evaluate the extent to which ECAP SOE patterns can be used to predict pitch discrimination ability for virtual channels.

The purpose of the present study was to systematically examine ECAP SOE functions for virtual-channel maskers and probes for a relatively large number of subjects that utilize two different methods to produce virtual channels: dual-electrode stimulation (newer Cochlear devices) and current steering (AB devices). Two experiments were conducted; Fig. 1 illustrates the general parameter of interest for each experiment. The goal of Experiment 1 was to determine whether ECAP SOE patterns differ for physical versus virtual *masker* electrodes. ECAP amplitudes were interpolated between adjacent physical masker electrodes to predict the amplitude obtained for an intermediate virtual-channel masker. Predicted amplitudes were then compared with measured amplitudes obtained for virtual-channel maskers. It was hypothesized that if virtual-channel stimulation with either dual-electrode mode (Cochlear) or a 50-50 current split (AB) between adjacent electrodes results in stimulation of an intermediate population of neurons, there would be no significant difference between predicted and measured amplitudes. However, if virtual-channel stimulation yields slightly larger amplitudes as demonstrated in Busby et al. (2008) and Hughes and Goulson (2011), then we expect that the predicted and measured amplitudes will differ significantly.

The goal of Experiment 2 was to evaluate whether the ECAP SOE patterns for a virtual-channel *probe* demonstrate measurable spatial separation from the patterns obtained for the adjacent physical electrodes. Although earlier studies suggested that ECAP SOE functions for virtual probe electrodes fall approximately half-way between the functions for adjacent physical electrodes, those results were based primarily on data from Cochlear recipients (using electrical coupling for dual-electrode stimulation), relatively small subject numbers (N = 9 or less), and non-replicated SOE functions that exhibited large variability across subjects (Busby et al., 2008; Hughes and Goulson, 2011). Only one study has empirically examined whether virtual-channel probe SOE patterns are significantly spatially separate

[1]Amplitudes for all SOE functions within a comparison set were normalized to the same value to avoid changing the spatial relationships between functions (i.e., the relative location of the edges of the SOE patterns). This issue is discussed further in the Methods.

from those of the flanking physical probe electrodes using current steering (AB devices; Snel-Bongers et al., 2012). In the present study, Experiment 2 further investigated the relation between virtual- and physical-probe-electrode SOE patterns in a larger group of subjects using two different mechanisms to achieve virtual-channel stimulation, and for whom SOE functions were replicated to reduce measurement variability. It was hypothesized that SOE patterns for a virtual-channel probe would yield a pattern that was significantly different from (i.e., spatially separate from) that of each of the two flanking physical electrodes. Further, it was expected that the amount of spatial separation between the physical-versus-virtual probe functions would be significantly smaller than that for the two adjacent physical probe electrodes. Last, the spatial separations between the virtual-channel probe and each of the flanking physical probes were expected to be similar.

2. Methods

2.1 Subjects

ECAP SOE functions were collected for 35 ears in 34 CI recipients: N=8 CII, N=11 HiRes 90K (AB, Sylmar, CA, USA), N=9 Nucleus 24RE(CA) Freedom, and N=7 Nucleus CI512 (Cochlear Ltd., Macquarie, NSW, Australia). The mean age at implant was 42 years, 5 months (range: 1 year, 9 months to 84 years, 7 months) and the mean duration of CI use at the time of participation was 3 years, 10 months (range: 3 months to 11 years). Additional demographic information is listed in Table 1. One subject was implanted bilaterally, indicated with asterisks in Table 1. Three subjects (bilateral subject F10/F11, N1, and N6) had been explanted and re-implanted; the duration of CI use in Table 1 reflects the total duration across both the explanted and replacement devices. Previous devices for F10, F11, N1, and N6 were a HiRes 90K, Clarion 1.2, Nucleus 24RE, and Nucleus 24RE, respectively. At the time of the study, F10/F11 had been using the 24RE devices for 1 year, 9 months in the right ear (F10) and 1 year, 2 months in the left ear (F11). N1 had used the CI512 for 2 years and N6 for 3 months. All subjects signed an informed consent prior to participating and were compensated for their time.

2.2 Equipment Setup

ECAPs for subjects with Cochlear devices were measured using the Advanced Neural Response Telemetry (NRT) feature within the Custom Sound EP software (v. 3.1 and 3.2) with the non-commercial “dual-electrode” feature enabled for research purposes. A laboratory Freedom speech processor was interfaced with a programming pod. ECAPs for AB subjects were measured with the Bionic Ear Data Collection System (BEDCS v1.18.295; Advanced Bionics Corp., Sylmar, CA), which is a non-commercial research platform that allows for custom stimulus and recording paradigms with AB devices. A laboratory Platinum Series Processor (PSP) was interfaced with a Clinical Programming Interface (CPI II) for data collection.

2.3 Stimuli

ECAPs were obtained using the standard four-frame forward-masking subtraction procedure described previously (e.g., Abbas et al., 2004; Hughes and Abbas, 2006). Briefly, the four frames consist of: (A) probe alone, (B) masker followed by probe, (C) masker alone, and (D) zero-amplitude pulse to obtain a template of the system artifact. The subtracted trace, A-B+C-D, yields the response to the probe. When the masker and probe are spatially separated, as with SOE functions, the resulting ECAP response represents the overlapping neural population that is recruited by both the masker and probe electrodes (Hughes and Abbas, 2006).

For Cochlear subjects, the following NRT stimulus parameters were used: 80 Hz probe rate; 25 or 50 μsec/phase pulse width, depending on voltage compliance limits (subjects F1, F5, F7, and N7 all used a pulse width of 50 μsec/phase); 7 μsec interphase gap; 400 μs masker-probe interval (MPI); and stimulating reference electrode MP1 (extracochlear monopolar ball electrode). The following recording parameters were used for Cochlear subjects: recording reference electrode MP2 (extracochlear monopolar case electrode), 50-100 sweeps, 50 dB gain, and 122 μsec recording delay (optimized individually as needed).

For AB subjects, the following stimulus parameters were used: 20 Hz probe rate, 32 μsec/phase pulse width (no interphase gap), 500 μsec MPI, and monopolar stimulating reference electrode (implant case). Virtual channels were achieved through simultaneous stimulation of adjacent electrode pairs with 50% of the total current delivered to each electrode in the pair. The following recording parameters were used: monopolar recording reference electrode (implant case for CII and extracochlear ring electrode for HiRes 90K), 80 averages, and 1000 gain (linear multiplier). With BEDCS, there is no recording delay parameter because recording begins prior to the end of the last stimulus pulse. For both Cochlear and AB devices, the recording electrode was typically located two electrodes apical to the probe. For virtual-channel probes, the recording electrode was two electrodes apical to the most basal electrode in the pair (this is the default configuration for Cochlear's dual-electrode mode). For some subjects, adjustments to the recording delay (Cochlear only), gain, and/or recording electrode were performed as needed to minimize stimulus artifact.

2.4 Procedures

Impedances were measured first to ensure that all test electrodes were functioning within the manufacturer's normal limits. Open circuits were measured for subject C15, electrode 16 and subject F2, electrode 8. Short circuits were measured for C19 on electrodes 9 and 14. None of these electrodes were used in the study.

Probe and masker presentation levels were determined by behavioral loudness estimates obtained at the beginning of the study. Ten sweeps of the ECAP stimulus were presented using an ascending approach that began at a level well below estimated threshold. Subjects were given a visual rating scale that ranged from "0" (no sound) to "10" (too loud) and were asked to indicate when they first heard the sound (rating of "1") and when the sound was loud (rating of "8"). Masker and probe stimuli for Experiment 1 were generally presented at a loudness rating of "8" except in cases where voltage compliance limits were reached or the subject experienced facial nerve stimulation. In these cases, the highest current level within compliance limits or that did not produce facial-nerve stimulation was used. For Experiment 2, "8" loudness ratings were initially obtained for each set of three probe electrodes. The lowest current level among the three probes that yielded an "8" was used for all three probes in the SOE functions that were compared. The rationale for this procedure is detailed below.

Loudness estimates were obtained for all physical electrodes and virtual channels listed in Table 2, as well as for the most apical and basal electrodes in the array. For example, loudness estimates for AB subjects were obtained for electrodes 1, 4, 4+5, 5, 8, 8+9, 9, 12, 12+13, 13, and 16 so that appropriate stimulus levels could also be determined for each masker. Linear interpolation was used to calculate masker presentation levels for the remaining electrodes for which loudness estimates were not measured. In addition to the electrodes listed in Table 2, loudness estimates for electrodes 9 and 15 were also measured for subjects with Cochlear devices so that levels were interpolated across no more than three adjacent electrodes.

ECAP SOE functions were obtained for the probe-electrode sets detailed in Table 2. Experiment 1 evaluated whether virtual-channel maskers yield ECAP amplitudes that are consistent with the rest of the SOE function. For this experiment, the probe was presented to one physical electrode (see Table 2, Experiment 1 and Fig. 1) while the masker was delivered to all physical electrodes (except the recording electrode) and all intermediate virtual channels across the array.

For Experiment 2, SOE functions for a virtual-channel probe were compared with the SOE functions for the two flanking physical probe electrodes (see Table 2, Experiment 2) to determine whether the virtual-channel SOE function demonstrated independent regions of excitation relative to the patterns obtained from the adjacent physical electrodes (see Fig. 1, bottom). For this experiment, maskers were delivered to all physical electrodes (except the recording electrode) and to the virtual-channel probe. SOE functions were measured twice for each stimulus condition to reduce measurement variability.

As with any evoked potential, stimulus level affects the overall ECAP amplitude. Amplitude normalization is often used to control for the use of different stimulus levels across probe electrodes so that SOE functions can be compared. Normalization typically involves dividing all amplitudes in each function by either the highest amplitude within each function (Busby et al., 2008) or the amplitude obtained with the masker and probe delivered to the same electrode (Hughes & Abbas, 2006). However, normalization can change the relative location of the edges of the patterns across SOE functions *if each function is normalized independently* (as demonstrated in Fig. 5 of Hughes and Goulson, 2011). This is problematic if the goal is to compare the spatial relationships among functions (i.e., relative location of pattern edges and peaks). However, if all amplitudes within a set of compared SOE functions (i.e. virtual channel and two flanking physical probes) are normalized *to a single value*, then the spatial relationships will not change (Hughes, 2008). This latter approach preserves the spatial relationships among functions, yet controls for differences in stimulus level and overall ECAP amplitude across subjects.

For Experiment 2, all probe electrodes within a set were tested using the same current level, initially to obviate the need for normalization (recall that normalization is typically used to control for differences in stimulus levels across compared SOE functions). If the “8” loudness ratings for the three probe electrodes in a set were different from each other, the lowest current level within the set was used for all three probes. It is important to note that categorical loudness ratings were used, which means that a range of current levels fall within the same category. For Cochlear and AB recipients, the average difference between the “8” rating and the level used for testing was 3.8 CL and 64.0 μA, respectively, which is smaller than the step size used for the loudness ratings in the upper portion of the dynamic range. Despite using equal probe levels within an electrode set, data for Experiment 2 were subsequently normalized to the single highest amplitude across all three probe functions within a set for each subject to allow for *cross-subject* comparisons (as in Hughes, 2008). With this method, the relative separation of SOE functions within a set could be preserved, while allowing for comparisons across electrode sets and subjects.

2.5 Data Analysis

ECAP amplitudes were calculated as the voltage difference between the N1 trough and P2 peak/plateau. For Cochlear subjects, peaks were marked by the automatic algorithmic in Custom Sound EP and were manually adjusted if necessary. For AB subjects, BEDCS data were read into a custom MATLAB (MathWorks Inc., Natick, MA) program where N1/P2 peaks were manually marked.

For Experiment 1, amplitudes for virtual-channel maskers were estimated using a linear fit between amplitudes for adjacent physical-electrode maskers in the SOE function. With a linear fit that assumes the virtual channel is produced with 50% current split between adjacent physical electrodes, the predicted ECAP amplitude for each virtual masker (A_V) is simply the average of the amplitudes for the adjacent physical masker electrodes (A_B and A_A, representing the basal and apical members of the pair, respectively):

$$A_V = (A_B + A_A)/2$$

Predicted and measured amplitudes were then compared for each virtual-channel masker.

For Experiment 2, spatial separation between each of the three functions (two adjacent probe electrodes and the intermediate virtual channel) in each cochlear region was quantified as the absolute value of the difference of the normalized amplitudes measured at each masker electrode, summed across all masker electrodes. The following formula from Hughes (2008) was used:

$$\sum_{i=1}^{j} |a_{xi} - a_{yi}|,$$

where a_x and a_y correspond to the normalized ECAP amplitudes of the two ECAP SOE functions being compared (probe electrode *x* versus *y*) for each masker electrode *i* (summed from 1 to *j*, where *j* is 16 for AB devices and 22 for Cochlear devices). The resulting value was termed the *separation index* (Σ). This method is illustrated in Fig. 4 and described further in the Results. Because ECAPs could not be recorded for maskers delivered to the recording electrode, interpolated amplitudes were used as a substitute for this condition. Similarly, interpolated amplitudes were used for electrodes with short or open circuits. It is important to note that Σ represents a summative value and therefore cannot be compared across devices that differ by number of electrodes and/or inter-electrode spacing. Devices with fewer electrodes (such as AB) will yield smaller Σ values, yet devices with electrodes that are spaced farther apart (also AB devices) will yield larger Σ values. These effects may counterbalance each other to some extent, but are nonetheless confounding effects that preclude direct comparisons across devices. Data for the present study were therefore analyzed separately by device type. A repeated-measures analysis of variance (RM ANOVA) with the factors electrode region and probe electrode pair was used to evaluate the spatial separation of SOE functions (Σ) for physical versus virtual probe electrodes.

3. Results

3.1 Experiment 1

Fig. 2 shows two individual examples of SOE functions (left column) for a Cochlear (Fig. 2A) and AB (Fig. 2C) subject. ECAP amplitudes for maskers delivered to physical electrodes (PM) and virtual channels (VM) are indicated by the larger black and white circles, respectively. Note that the amplitudes for the virtual-channel maskers (white circles) generally fell between those for the adjacent physical electrodes for both subjects. Predicted amplitudes for virtual-channel maskers are indicated by the smaller circles. The right column (Figs. 2B and 2D) shows corresponding scatter plots that compare the predicted and measured ECAP amplitudes for the virtual-channel maskers. For both subjects, the measured amplitudes closely approximated the predicted amplitudes. Pearson correlation coefficients were $r = 1.0$ ($p < 0.001$) and 0.997 ($p < 0.001$) for subjects F4 and C14, respectively.

However, paired t-tests showed that the average measured amplitudes for the virtual-channel maskers were significantly higher (~6 μV) than those predicted by the physical electrodes for Cochlear subject F4 ($p = 0.005$, 2-tailed). There was no significant difference for AB subject C14 ($p = 0.051$).

To determine whether the predicted and measured ECAP amplitudes were equivalent across the group data, predicted amplitudes were subtracted from the measured amplitudes for each virtual-channel masker condition to obtain a difference value. One-sample signed rank tests (due to non-normal distribution of data) were used to test the hypothesis that the difference between predicted and measured values would not differ significantly from the expected value of zero. Figure 3 shows box-and-whisker plots of the amplitude difference for the three probe regions (basal, middle, apical), separated by device type (Cochlear, top; AB, bottom). Data for the basal probe for subjects C15, C28, and C40 were not available because no measurable ECAP responses could be obtained (see Table 1). Additionally, data for subject C29 were excluded because her ECAPs were more than an order of magnitude larger than the other subjects' (~2000 μV), resulting in amplitude differences that were also more than an order of magnitude larger than that of the group data.

For Cochlear subjects, the median amplitude difference was significantly different from the expected value of zero for all three probe regions ($z = 3.4$, $p < 0.001$ for basal, $z = 5.8$, $p < 0.001$ for middle, and $z = 4.9$, $p < 0.001$ for apical). All comparisons were significant using an adjusted p for multiple comparisons ($p = 0.015$). Overall, measured amplitudes were significantly larger than the predicted amplitudes ($z = 8.23$, $p < 0.001$; Wilcoxon signed rank test). However, the mean differences were small: 121.28 μV (SD = 156.81) for measured versus 119.44 μV (SD = 154.81) for predicted. For AB subjects, there was no significant difference between the median amplitude difference and the expected value of zero ($z = 1.3$, $p = 0.19$ for basal, $z = -0.2$, $p = 0.87$ for middle, and $z = 0.2$, $p = 0.85$ for apical). Measured and predicted amplitude means were 114.30 μV [SD = 156.26] and 112.79 μV [SD = 152.22], respectively).

3.2 Experiment 2

For Experiment 2, two replications of ECAP SOE functions were averaged together to reduce measurement variability for the comparison between physical and virtual-channel probe functions. Following the method described in Hughes (2008), the separation index between adjacent SOE functions and the intermediate virtual-channel function were calculated. Two individual examples are shown in Fig. 4. Normalized data for Cochlear subject F4 and AB subject C29 are displayed in the top and bottom panels, respectively. SOE functions for the two adjacent probes are shown with filled circles (basal-most probe) and filled triangles (apical-most probe); the intermediate virtual-channel probe is shown with open squares. Within each subject, all amplitudes were normalized to the single highest amplitude across all three probe sets, as described in the Methods. In both examples shown in Fig. 4, SOE functions for the virtual-channel probes were spatially located between the two physical-probe-electrode SOE functions. At each masker electrode, dotted or solid lines indicate the spatial separation between the virtual-channel function and the basal-side probe or the apical-side probe, respectively. For subject F4, the separation index was $\Sigma = 0.77$ between the P11 and P11+12 functions and $\Sigma = 0.98$ between the P11+12 and P12 functions, which means the P11+12 function was more spatially separate from the P12 function than the P11 function. In other words, the virtual-channel function was weighted slightly toward the more basal electrode in the pair (P11). For subject C29, the separation index was $\Sigma = 1.01$ between the P9 and P8+9 functions, and $\Sigma = 1.00$ between the P8 and P8+9 functions, which means the virtual-channel probe function was essentially equidistant between those of the two physical probe electrodes.

Fig. 5 shows the group separation-index data for Cochlear (white) and AB (gray) subjects for each probe-electrode SOE comparison. Results for basal, middle, and apical electrode sets are displayed from top to bottom, respectively. Within each panel, the pairs of box-and-whisker plots represent comparisons between the basal-most probe in the pair and the virtual-channel probe (left grouping), the virtual-channel probe and the apical-most probe in the pair (center grouping), and the basal-most versus apical-most probe in the pair (right grouping) for each device type. Box boundaries represent the 25^{th} and 75^{th} percentiles, whiskers represent the 10^{th} and 90^{th} percentiles, black circles represent outliers, and horizontal solid and dashed lines represent medians and means, respectively.

A two-way RM ANOVA was used to examine the effects of electrode region (basal, middle, apical) and comparison pair (basal-most vs. virtual, virtual vs. apical-most, basal-most vs. apical-most) on the separation index for each device type separately. Table 3 summarizes the mean Σ values across region and comparison pair (within each region) for both device types. Results for Cochlear subjects showed significant main effects for region [$F(2, 28) = 3.42$, $p = 0.047$], comparison pair [$F(2, 28) = 14.65$, $p < 0.001$], and region*pair interaction [$F(4, 56) = 2.82$, $p = 0.033$]. Bonferonni adjustments were made for all post-hoc pairwise comparisons. For the main effect of region, post-hoc comparisons showed no significant difference in Σ values across regions, although the difference between the mean middle and apical Σ values approached significance ($p = 0.052$). Mean Σ values were smallest for the apical set (Σ = 1.12), followed by the basal set (Σ = 1.50), with the middle set (Σ = 1.59) having the largest separation index (see Table 3).

For the main effect of comparison pair, post-hoc pairwise comparisons showed significant differences between both virtual-channel comparisons and the basal-apical (physical electrode) comparisons ($p < 0.02$). There was no significant difference between the basal-virtual and virtual-apical Σ values (p = 0.06). On average, Σ values were largest for the basal-apical (physical electrode) comparison (Σ = 1.68), followed by the virtual-apical comparison (Σ = 1.35), and finally the basal-virtual comparison (Σ = 1.17). These results indicate greater spatial separation between adjacent physical-probe SOE functions than between the virtual-channel function and either of the flanking physical probes, as expected. Although not statistically significant, the spatial separation for the basal-virtual comparisons were consistently smaller than the virtual-apical comparisons across regions, suggesting a slight bias of the virtual-channel SOE function toward the basal electrode in each pair.

Finally, for the region*pair interaction, both virtual-channel comparison pairs (basal-virtual and virtual-apical) within the middle region had significantly smaller Σ values than the respective basal-apical comparison ($p < 0.001$), as expected. These results support the hypothesis that SOE functions for adjacent physical probe electrodes are more spatially separate than SOE functions for a physical probe and the intermediate virtual channel. For the basal region, only the basal-virtual comparison was significantly smaller than the basal-apical comparison (p < 0.001), supporting the notion that the virtual-channel SOE function is weighted slightly toward the basal electrode in the pair. For the apical region, none of the Σ values differed significantly.

For AB data, the assumption of sphericity was not met for comparison pair [Mauchly's $W(2) = 0.36$, $p = 0.001$] or region*pair interaction [$W(9) = 0.21$, $p = 0.01$]. Therefore, Greenhouse-Geisser Epsilon values of 0.61 and 0.55 were used to adjust the degrees of freedom for comparison pair and region*pair, respectively. Results showed a significant main effect for comparison pair [$F(1.22, 30) = 42.56$, $p < 0.001$]. There was no significant effect of region [$F(2, 30) = 2.30$, $p = 0.12$] or region*pair interaction [$F(2.22, 60) = 2.65$, $p = 0.08$]. Mean Σ values across region were similar to the trends exhibited by the Cochlear

data; Σ was smallest for the apical set (Σ = 1.35), followed by the basal set (Σ = 1.78), with the middle set (Σ = 1.85) having the largest separation index (see Table 3).

For the main effect of comparison pair, trends were again similar to those exhibited by the Cochlear data. Post-hoc pairwise comparisons showed significant differences between both virtual-channel comparisons and the basal-apical (physical electrode) comparisons ($p < 0.001$). There was no significant difference between the basal-virtual and virtual-apical Σ values (p = 0.08). On average, Σ values were largest for the basal-apical (physical electrode) comparison (Σ = 2.20), followed by the virtual-apical comparison (Σ = 1.57), and finally the basal-virtual comparison (Σ = 1.22). As with the Cochlear data, the spatial separation for the basal-virtual comparisons in AB subjects were consistently smaller than the virtual-apical comparisons across regions, again suggesting a slight bias of the virtual-channel SOE function toward the basalelectrode in each pair (see Table 3).

4. Discussion

This study systematically evaluated ECAP SOE functions for virtual-channel maskers and probes in two experiments. Experiment 1 investigated whether virtual channel maskers yield amplitudes consistent with those interpolated from physical electrodes. It was expected that the measured and predicted amplitudes would not be significantly different. Experiment 2 quantified the amount of spatial separation between SOE functions obtained with virtual-channel and adjacent physical-electrode probes. It was expected that: (1) SOE patterns for a virtual-channel probe would be spatially separate from that of each of the two flanking physical electrodes, (2) the amount of spatial separation between the physical-virtual probe functions would be significantly less than for the two adjacent physical probe electrodes, and (3) the spatial separation between the virtual-channel probe and each of the flanking physical probes would be similar.

4.1 Experiment 1

Results from Experiment 1 (see Fig. 3) revealed no significant difference between predicted and measured ECAP amplitudes for AB subjects, consistent with the hypothesis. For a group of AB subjects, Saoji et al. (2009) utilized a virtual-channel masker with a 50% current-steering split between non-adjacent electrodes to obtain ECAP SOE functions. They found no difference in the area under the curve or peak of the function (center of gravity) relative to functions obtained with the masker delivered to the intermediate physical electrode. Their study, however, used a fixed masker electrode with varied probe electrodes, which is opposite the method used in the present and other previous studies. Thus, their results with a virtual-channel masker are more comparative to virtual-channel probe results (e.g., Experiment 2 of the present study; Busby et al., 2008). Further, the virtual-channel masker in Saoji et al. was produced using simultaneous stimulation of two *non-adjacent* electrodes (e.g., E6+E8) and results were compared with measured amplitudes from the intermediate physical electrode (e.g., E7). In contrast, the present study used amplitudes interpolated from adjacent physical electrodes to compare with measured amplitudes obtained with intermediate virtual-channel maskers. Despite the inherent differences in methodology between the two studies, the present results from AB subjects concur with those of Saoji et al. (2009) in that stimulation with virtual-channel maskers yield similar results to those obtained or interpolated from physical electrodes.

In contrast to the AB data, measured ECAP amplitudes for virtual-channel maskers were significantly larger for Cochlear subjects than the predicted amplitudes that were interpolated from the adjacent physical masker electrodes. This result is consistent with the alternative hypothesis that slightly larger amplitudes result from dual- than single-electrode stimulation (Busby et al., 2008; Hughes & Goulson, 2011). Because the mechanisms used to

achieve virtual channels differ between devices, it may be that electrical coupling yields slightly broader regions of excitation than current steering. With current steering, the respective electrical fields from each electrode sum together to form the virtual channel. In some cases, small portions of each field may not overlap enough to fully sum, yielding a smaller overall excitation region than that produced with electrical coupling. This theory is supported by the data in Fig. 3 (greater number and range of negative amplitude difference measures for AB subjects) and earlier studies that reported slightly higher current levels were needed for current steering to yield equal loudness relative to each physical electrode alone for some subjects (e.g., Donaldson et al., 2005). For electrical coupling, Busby et al. (2008) examined the widths of SOE functions for single- and dual-electrode stimulation and found no significant difference between the two. They noted, however, that the higher amplitudes observed for dual-electrode stimulation may not be large enough to translate into broader SOE functions. In sum, although the amplitude differences between measured and predicted values for Cochlear recipients were statistically significant, they were relatively small. Measured amplitudes were, on average, <2 μV larger than the predicted amplitudes. Given that the amplifier noise floor is approximately 2 μV for the Nucleus 24RE and CI512 devices (Patrick et al., 2006), the differences observed in the present study are likely notclinically significant.

4.2 Experiment 2

Results from Experiment 2 (see Fig. 5) showed no significant differences across electrode regions; however, the apical probe set yielded the least amount of spatial separation amongst the virtual- and physical-probe SOE functions, followed by the basal probe set (see Table 3). The maximum separation between the masker and probe electrodes along the length of the array differs across the electrode sets tested. For a probe electrode in the middle of the array the maximum separation between the probe and the farthest masker electrode will be roughly half of the length of the implanted array (i.e., a distance of 7-8 electrodes for AB or 10-11 electrodes for Cochlear). However, for a basal or apical probe, the distance between the probe and the farthest masker electrode will be nearly the entire length of the array (i.e., for this study, 11-12 electrodes for AB or electrodes for Cochlear). Recall that with the forward-masking subtraction method, ECAP amplitudes in the SOE function reflect the relative overlap of neural populations responding to the masker and probe (Hughes & Abbas, 2006). Thus, for larger masker-probe separations, there is less overlap, resulting in diminished ECAPs or zero-amplitude measures. For probes located at either end of the array, the separation index will likely include more zero-amplitude measures because of the larger masker-probe separations, resulting in a smaller Σ value. For a probe in the middle of the array, however, there are likely to be more observations with measurable responses that collectively contribute to a larger separation index, as evidenced by the data in Table 3.

Differences in nerve survival patterns across the cochlea may have also contributed to the small differences in mean Σ values across the electrode regions. Specifically, if there is greater variation in nerve survival patterns across adjacent electrodes, then the overall ECAP amplitudes are likely to be substantially different for a fixed current level (as used in the present study), lending to larger Σ values. An example is illustrated in Fig. 6, which shows normalized SOE functions for the basal, middle, and apical electrode sets (top to bottom, respectively) for subject C19. For the basal and middle electrode sets, there are relatively large amplitude differences between the adjacent physical-probe functions, whereas the SOE functions for the apical set are more uniform. The uniform SOE patterns for the apical set may reflect more uniform nerve survival patterns. Last, the tapered shape of the cochlea toward the apex and closer spacing of electrode contacts toward the apical end of the array may have also contributed to the reduced separation among apical SOE functions.

The analyses for both devices (Fig. 5) showed significantly larger Σ values for the comparison between the adjacent physical probe SOE functions (basal-apical comparison), as expected. Further, the results are consistent with the hypothesis that a virtual-channel probe yields an SOE function that is spatially separate from that of each of the two flanking physical electrodes. The results also support the hypothesis that the spatial separation between the physical and virtual probe functions is significantly smaller than the spatial separation between the two adjacent physical probe electrodes. Additional studies are currently underway in our laboratory that compare the ECAP SOE spatial separation indices (Σ) to psychophysical measures of pitch ranking and electrode discrimination to examine the extent to which Σ values can predict pitch resolution for virtual-channel stimulation.

Although not statistically significant, the mean Σ value for the virtual-apical comparison was consistently larger than the mean for the basal-virtual comparison across devices and probe regions, which suggests that the SOE function for the virtual-channel probe tended to be weighted more toward the basal-most electrode in the pair. An example is shown in the middle panel of Fig. 6. Given the assumption that current was equally distributed between the two adjacent probe electrodes, the Σ values for the two virtual-channel comparisons were expected to be similar. As noted above, uneven patterns of neural survival could produce larger differences in SOE functions for adjacent probe electrodes (Nadol, 1997). SOE functions may be more likely to overlap if they recruit a similar population of neurons. A denser neural population located toward the apical side of the more apical physical electrode in this example may contribute to a larger SOE function for the apical probe in the pair, but that denser population may be outside the spatial reach of the virtual-channel or basal-most probes.

In sum, this study showed that virtual-channel maskers yield ECAP amplitudes for SOE functions that are generally consistent with (AB) or slightly larger than (Cochlear) the amplitudes obtained with stimulation of physical electrodes. When the spatial separation between virtual-channel and flanking physical-electrode SOE functions were examined across the three electrode regions, the apical probe set demonstrated the least amount of spatial separation. This finding may be the result of more uniform patterns of nerve survival in the apical region and/or the tapered geometry of the cochlea. In general, there was greater spatial separation between SOE functions for adjacent physical probes than for comparisons between each physical probe and the intermediate virtual channel, as expected. Finally, the virtual-channel functions tended to be weighted more toward the basal electrode in the pair.

Acknowledgments

This research was supported by NIH/NIDCD grants R01 DC009595 and P30 DC04662. The content of this project is solely the responsibility of the authors and does not necessarily represent the official views of the National Institute on Deafness and Other Communication Disorders or the National Institutes of Health. The authors thank Donna Neff, Adam Goulson, Katelyn Glassman, and Gina Diaz for assistance with data collection; Tom Creutz for data-analysis programs; Kanae Nishi for statistical assistance; Bas Van Dijk (Cochlear Europe) and Peter Busby (Cochlear Australia) for Custom-Sound EP Dual Electrode support; and Leo Litvak and Aniket Saoji (Advanced Bionics) for BEDCS support.

Abbreviations

AB	Advanced Bionics
BEDCS	Bionic Ear Data Collection System
CI	cochlear implant
CL	current level units

ECAP	electrically evoked compound action potential
MPI	masker-probe interval
NRT	Neural Response Telemetry
pps	pulses per second
SD	standard deviation
SOE	spread of excitation
PSP	Platinum Series Processor
CPI II	Clinical Programming Interface
PM	physical-electrode maskers
RM ANOVA	repeated-measures analysis of variance
VM	virtual-channel maskers

REFERENCES

Abbas PJ, Brown CJ, Shallop JK, Firszt JB, Hughes ML, Hong SH, Staller SJ. Summary of results using the Nucleus CI24M implant to record the electrically evoked compound action potential. Ear Hear. 1999; 20:45–59. [PubMed: 10037065]

Abbas PJ, Hughes ML, Brown CJ, et al. Channel interaction in cochlear implant users evaluated using the electrically evoked compound action potential. Audiol. Neurotol. 2004; 9:203–213.

Bonham, B. H. & Litvak; L, M. Current focusing and steering: modeling, physiology, and psychophysics. Hear Res. 2008; 242:141–153. [PubMed: 18501539]

Busby PA, Battmer RD, Pesch J. Electrophysiological spread of excitation and pitch perception for dual and single electrodes using the Nucleus Freedom cochlear implant. Ear Hear. 2008; 29(6):853–864. [PubMed: 18633324]

Busby PA, Plant KL. Dual electrode stimulation using the Nucleus CI24RE cochlear implant: Electrode impedance and pitch ranking studies. Ear Hear. 2005; 26:504–511. [PubMed: 16230899]

Choi CTM, Hsu C-H. Conditions for generating virtual channels in cochlear prosthesis systems. Ann. Biomed. Eng. 2009; 37:614–624. [PubMed: 19085105]

Donaldson GS, Kreft HA, Litvak L. Place-pitch discrimination of single-versus dual-electrode stimuli by cochlear implant users. J Acoust Soc Am. 2005; 118(2):623–626. [PubMed: 16158620]

Firszt JB, Burton-Koch D, Downing M, Litvak L. Current steering creates additional pitch percepts in adult cochlear implant recipients. Otol. Neurotol. 2007; 28:629–636. [PubMed: 17667771]

Frijns JHM, Kalkman RK, VanPoucke FJ, Snel Bongers J, Briaire JJ. Simultaneous and non-simultaneous dual electrode stimulation in cochlear implants: evidence for two neural response modalities. Acta. Oto-Laryngol. 2009; 129:433–439.

Henry BA, Turner CW. The resolution of complex spectral patterns by cochlear implant and normal-hearing listeners. J. Acoust. Soc. Am. 2003; 113(5):2861–2873. [PubMed: 12765402]

Henry BA, Turner CW, Behrens A. Spectral peak resolution and speech recognition in quiet: Normal hearing, hearing impaired, and cochlear implant listeners. J. Acoust. Soc. Am. 2005; 118(2):1111–1121. [PubMed: 16158665]

Hughes ML. A re-evaluation of the relation between physiological channel interaction and electrode pitch ranking in cochlear implants. J. Acoust. Soc. Am. 2008; 124(5):2711–2714. [PubMed: 19045758]

Hughes ML, Abbas PJ. The relation between electrophysiologic channel interaction and electrode pitch ranking in cochlear implant recipients. J. Acoust. Soc. Am. 2006; 119:1527–1537. [PubMed: 16583898]

Hughes ML, Goulson AM. Electrically evoked compound action potential measures for virtual channels versus physical electrodes. Ear Hear. 2011; 32:323–330. [PubMed: 21187752]

Koch DB, Downing M, Osberger MJ, Litvak L. Using current steering to increase spectral resolution in CII and HiRes 90K users. Ear Hear. 2007; 28:38S–41S. [PubMed: 17496643]

Kwon BJ, van den Honert C. Dual-electrode pitch discrimination with sequential interleaved stimulation by cochlear implant users. J. Acoust. Soc. Am. 2006; 120(1):EL1–EL6. [PubMed: 16875252]

McDermott HJ, McKay CM. Pitch ranking with nonsimultaneous dual-electrode electrical stimulation of the cochlea. J. Acoust. Soc. Am. 1994; 96:155–162. [PubMed: 8064018]

McKay CM, McDermott HJ, Clark GM. The perceptual dimensions of single-electrode and nonsimultaneous dual-electrode stimuli in cochlear implantees. J. Acoust. Soc. Am. 1996; 99:1079–1090. [PubMed: 8609291]

Nadol JB Jr. Patterns of neural degeneration in the human cochlea and auditory nerve: Implications for cochlear implantation. Otol. Head Neck Surg. 1997; 117:220–228.

Patrick JF, Busby PA, Gibson PJ. The development of the Nucleus® Freedom™ cochlear implant system. Trends Amplif. 2006; 10(4):175–200. [PubMed: 17172547]

Saoji AA, Litvak LM, Hughes ML. Excitation patterns in simultaneous and sequential dual-electrode stimulation in cochlear implant recipients. Ear Hear. 2009; 30:559–567. [PubMed: 19617837]

Snel-Bongers J, Briaire JJ, Vanpoucke FJ, Frijns JHM. Spread of excitation and channel interaction in single- and dual-electrode cochlear implant stimulation. Ear Hear. 2012; 33:367–376. [PubMed: 22048258]

Highlights

- Excitation patterns for virtual-channel maskers are similar to those for physical electrodes.
- Apical electrodes had the least amount of spatial separation among SOE functions.
- Virtual-channel functions were biase toward the basal-side electrode in the physical pair.

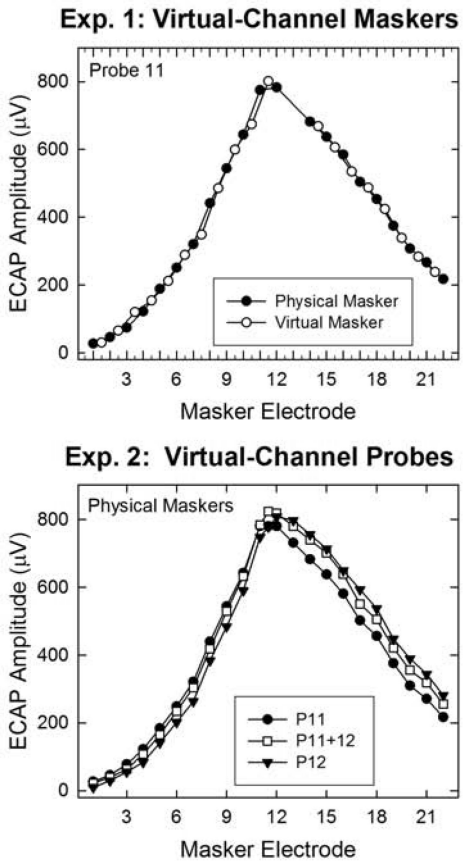

Fig. 1.

Individual examples illustrating the goal of each experiment. Experiment 1 (top) examined whether ECAP amplitudes obtained with virtual-channel maskers (open circles) were consistent with estimated values from maskers applied to physical electrodes (filled circles). Experiment 2 (bottom) examined the spatial separation between SOE patterns for adjacent physical probe electrodes (filled symbols) versus the intermediate virtual channel (open squares). Data are from subject F5.

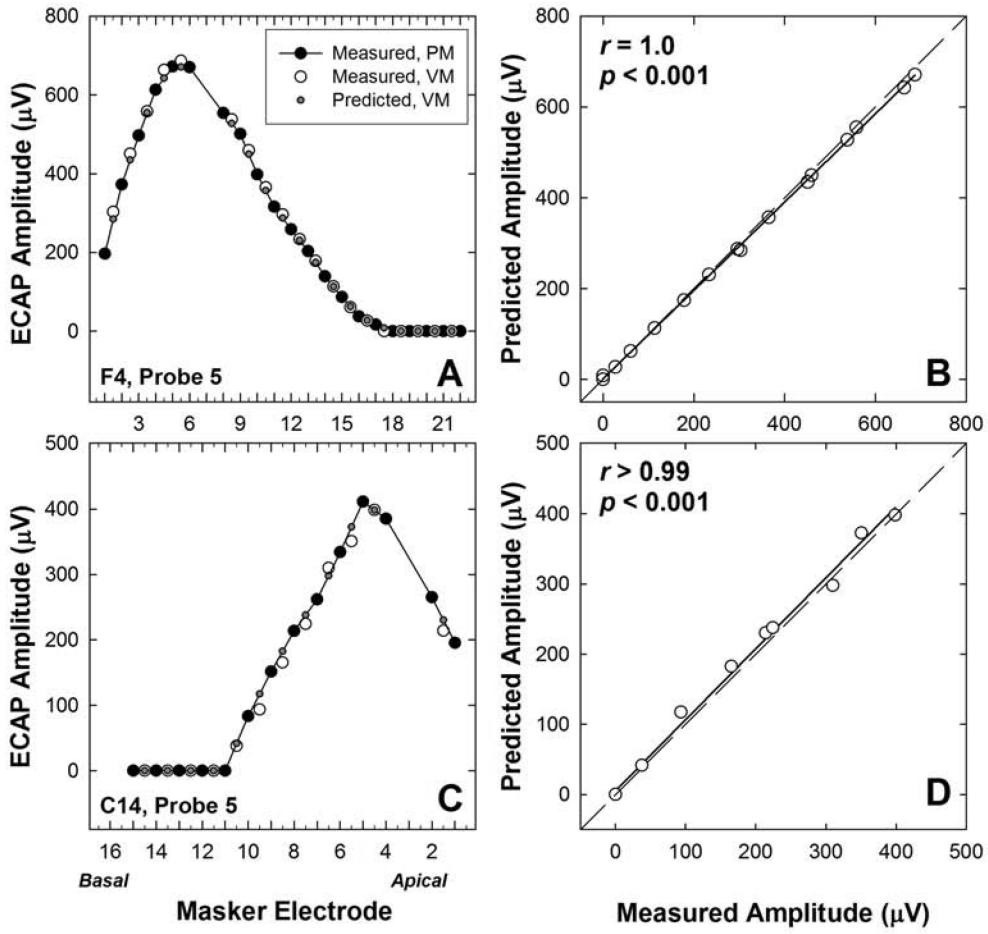

Fig. 2.

A and C: ECAP spread-of-excitation patterns for subjects F4 and C14, respectively. Measured amplitudes for physical-electrode maskers (PM) and virtual-channel maskers (VM) are shown with larger black and white circles, respectively. Predicted amplitudes for the virtual-channel maskers are shown with smaller gray circles. Subject number and probe electrode are indicated in each panel. B and D: Corresponding scatter plots comparing predicted versus measured amplitudes for virtual-channel maskers. Correlation coefficients (Pearson's *r*) and *p*-values are shown in each graph. Regression lines are shown with shorter, solid lines. The diagonal dashed line represents unity.

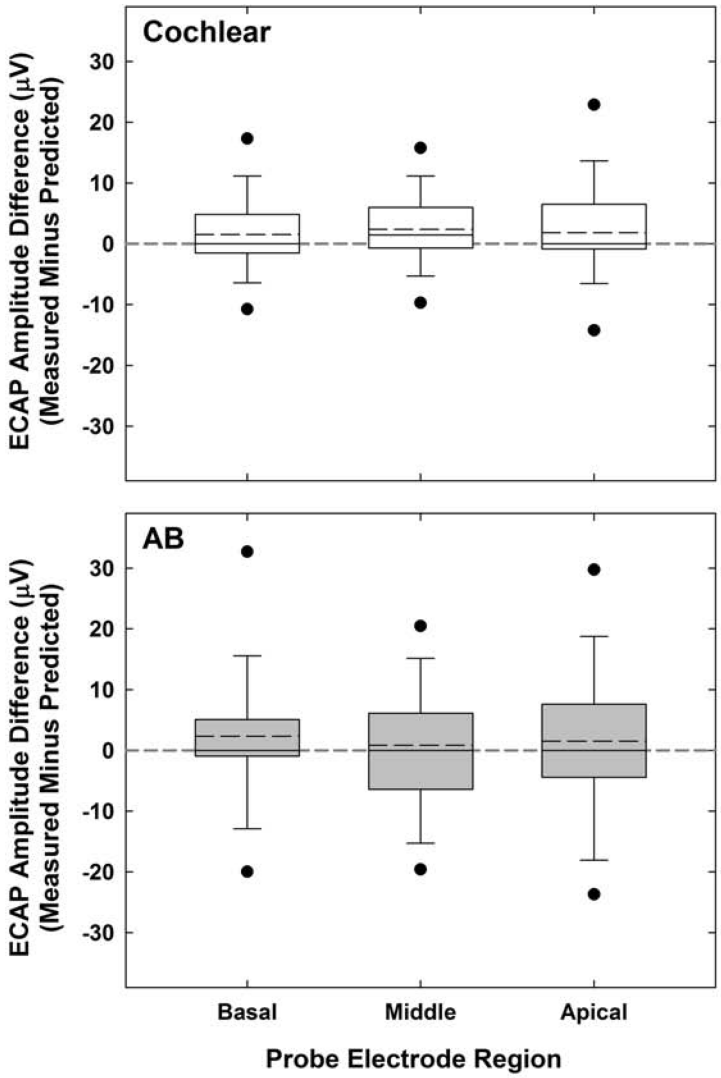

Fig. 3.

Group data showing measured minus predicted ECAP amplitudes for all virtual-channel maskers for Cochlear (top) and AB (bottom) subjects, each separated by probe electrode region. Box boundaries represent 25th and 75th percentiles; whiskers, 10th and 90th percentiles; black circles, 5th and 95th percentiles; horizontal solid lines, medians; and horizontal long dashed lines, means. The gray horizontal short-dashed line extending the length of each graph represents the expected amplitude difference of zero.

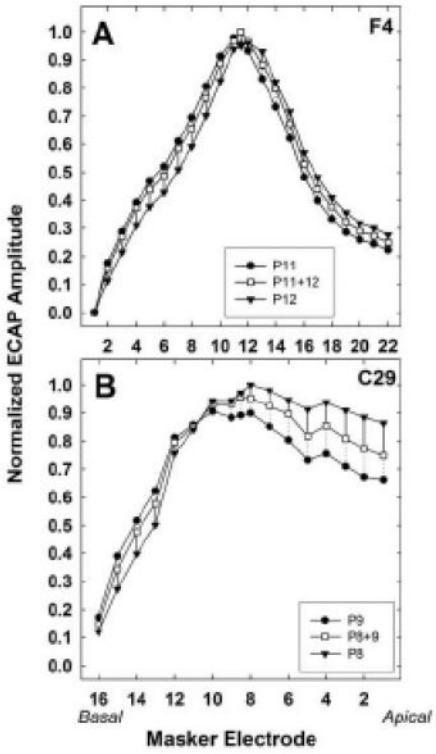

Fig. 4.

Normalized SOE functions for Cochlear subject F4 (top) and AB subject C29 (bottom). Filled circles, basal-most probe; filled triangles, apical-most probe; open squares, intermediate virtual-channel probe. For each subject, all amplitudes were normalized to the single highest amplitude across all three probe sets. Dotted or solid lines represent the spatial separation between the virtual-channel function and the basal-side probe or the apical-side probe, respectively.

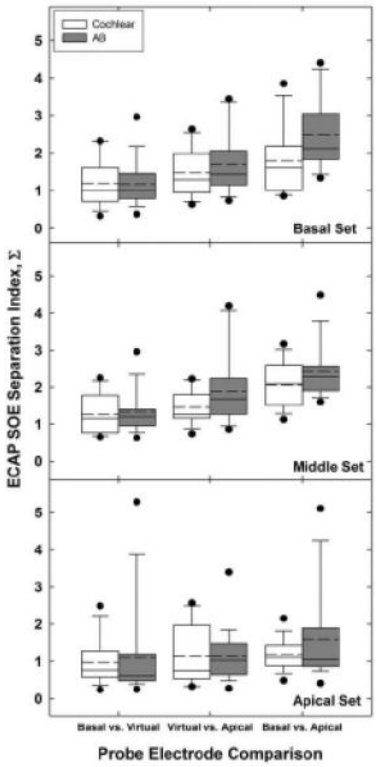

Fig. 5.

Group separation index data (Σ) for Cochlear (white bars) and AB (gray bars) subjects. Basal, middle, and apical probe-electrode sets are shown from top to bottom, respectively. Within each panel and device type, three comparisons for each electrode set are shown: basal-most vs. virtual probe functions (left grouping), virtual vs. apical-most probe functions (middle grouping), and basal-most vs. apical-most physical probe functions (right grouping). Boxes represent 25th and 75th percentiles; whiskers, 10th and 90th percentiles; black circles, outliers; horizontal solid lines, medians; and horizontal dashed lines, means.

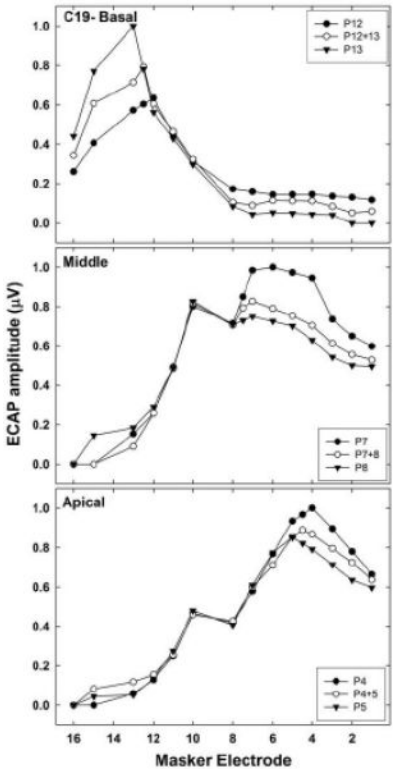

Fig. 6.

Normalized SOE functions for basal (top), middle (middle), and apical (bottom) electrode sets for AB subject C19, illustrating relative differences between functions within each region. Probe electrodes are identified in each figure legend.

Table 1

Demographic information for participants. *Each ear for the subject with bilateral CIs. ^Total duration of CI use; subject had been explanted and reimplanted. HF = HiFocus array, L = left, R = right, SNHL = sensorineural hearing loss, NR = no response for any electrode in that region.

Subject	Internal Device and Electrode Array	Ear	Age at CI (yrs, mos)	Dur CI Use (yrs, mos)	Dur Deafness (yrs or yrs, mos)	Etiology (Time course)	Electrode Set (Basal, Middle, Apical)
C1	Clarion CII HF 1 + positioner	R	18, 4	6, 11	Unknown	Unknown (Progressive)	12/13, 8/9, 4/5
C8	Clarion CII HF 1J	L	55, 7	5, 8	3	Unknown (Sudden SNHL)	12/13, 8/9, 4/5
C13	Clarion CII HF 1J	L	77, 1	6, 5	3+	Unknown-Familial	12/13, 8/9, 4/5
C14	Clarion CII HF 1J	R	6, 2	8, 3	0, 2	Pendred Syndrome (Progressive)	12/13, 8/9, 4/5
C15	HiRes 90K HF 1J	L	39, 3	4, 8	Unknown	Unknown	NR, 8/9, 4/5
C17	HiRes 90K HF 1J	R	7, 1	4, 5	5	Enlarged Vestibular Aquaducts	12/13, 8/9, 4/5
C19	HiRes 90K HF 1J	R	15, 5	5, 3	0, 4	Unknown (Sudden from established SNHL)	12/13, 7/8, 4/5
C22	HiRes 90K HF 1J	L	15, 4	1, 4	15+	Unknown-Familial (Progressive)	12/13, 8/9, 4/5
C23	Clarion CII HF 1 + positioner	L	69, 11	7, 6	Unknown	Unknown-Familial (Progressive)	12/13, 8/9, 4/5
C24	Clarion CII HF 1 + positioner	R	67, 4	8, 1	15	Unknown (Progressive)	12/13, 8/9, 4/5
C25	HiRes 90K HF 1J	L	11, 6	5, 3	Unknown	Usher Syndrome	12/13, 8/9, 4/5
C26	HiRes 90K HF 1J	R	67, 6	1, 10	27	Unknown	12/13, 8/9, 4/5
C28	HiRes 90K HF 1J	L	17, 0	0, 7	2	Oculo-auriculo-vertebral syndrome	NR, 8/9, 4/5
C29	HiRes 90K HF 1J	R	31, 0	2, 7	2	Meningitis	12/13, 8/9, 4/5
C32	HiRes 90K HF 1J	L	76, 9	4, 11	8	Unknown-Familial	12/13, 8/9, 4/5
C34	Clarion CII HF 1 + positioner	R	5, 10	9, 9	5	Unknown (Congenital)	12/13, 8/9, 4/5
C35	HiRes 90K HF 1J	R	84, 7	2, 2	4	Unknown (Sudden from established SNHL)	12/13, 8/9, 4/5
C39	HiRes 90K HF 1J	R	63, 0	3, 3	0, 6	Unknown	12/13, 8/9, 4/5
C40	Clarion CII HF 1 + positioner	L	59, 5	10, 9	21	Unknown-Familial (Progressive)	NR, 8/9, 4/5
F1	Nucleus 24RE (CA)	L	60, 7	2, 6	54	Unknown	5/6, 11/12, 17/18
F2	Nucleus 24RE (CA)	R	60, 2	1, 9	10	Unknown	5/6, 11/12, 17/18
F4	Nucleus 24RE (CA)	L	17, 6	1, 6	17	Ototoxicity	5/6, 11/12, 17/18
F5	Nucleus 24RE (CA)	R	48, 3	0, 11	7	Unknown	4/5, 11/12, 18/19
F6	Nucelus 24RE (CA)	R	31, 0	4, 10	Unknown	Unknown	5/6, 11/12, 17/18
F7	Nucleus 24RE (CA)	R	39, 1	2, 3	28	Unknown	5/6, 11/12, 18/19
F10*	Nucleus 24RE (CA)	R	8, 3	4, 7^	8, 3	Waardenburg Syndrome	5/6, 11/12, 17/18
F11*	Nucleus 24RE (CA)	L	1, 9	11, 0^	1, 10	Waardenburg Syndrome	5/6, 11/12, 17/18
F15	Nucleus 24RE (CA)	L	22, 10	1, 10	22, 9	Unknown (Congenital)	5/6, 11/12, 17/18
N1	Nucleus CI512	L	58, 3	1, 1^	8	Unknown-Familial, Noise	5/6, 11/12, 17/18
N2	Nucleus CI512	R	68, 3	0, 7	5	Usher Syndrome	5/6, 11/12, 17/18
N4	Nucleus CI512	R	13, 4	0, 11	0, 6	Unknown	5/6, 11/12, 17/18

Subject	Internal Device and Electrode Array	Ear	Age at CI (yrs, mos)	Dur CI Use (yrs, mos)	Dur Deafness (yrs or yrs, mos)	Etiology (Time course)	Electrode Set (Basal, Middle, Apical)
N5	Nucleus CI512	R	50, 9	0, 3	1	Unknown (Sudden SNHL)	5/6, 11/12, 17/18
N6	Nucleus CI512	R	83, 8	1, 10^	4	Unknown (Progressive)	5/6, 11/12, 17/18
N7	Nucleus CI512	R	69, 9	0, 5	10+	Unknown (Progressive)	5/6, 11/12, 17/18
N11	Nucleus CI512	L	67, 5	0, 3	6	Unknown (Progressive)	5/6, 11/12, 17/18

Table 2

Probe-electrode sets by device for spread-of-excitation functions obtained for Experiments 1 and 2.

	Experiment 1		Experiment 2	
Region	**Cochlear Probe Electrode**	**Advanced Bionics Probe Electrode**	**Cochlear Probe Electrode Set**	**Advanced Bionics Probe Electrode Set**
Basal	5	13	5, 5+6, 6	13, 12+13, 12
Middle	11	9	11, 11+12, 12	9, 8+9, 8
Apical	17	5	17, 17+18, 18	5, 4+5, 4

Table 3

Mean separation indices (Σ) for each probe region (collapsed across comparison pairs) and comparison pair (within each region), separated by device. BV, basal-virtual pair; VA, virtual-apical pair; BA, basal-apical pair.

Region	Mean Σ		Pair	Mean Σ	
	Cochlear	AB		Cochlear	AB
Basal	1.50	1.78	Basal-Virtual	1.23	1.17
			Virtual-Apical	1.46	1.69
			Basal-Apical	1.81	2.49
Middle	1.59	1.85	Basal-Virtual	1.27	1.34
			Virtual-Apical	1.46	1.84
			Basal-Apical	2.06	2.39
Apical	1.12	1.35	Basal-Virtual	1.02	1.15
			Virtual-Apical	1.14	1.18
			Basal-Apical	1.19	1.71